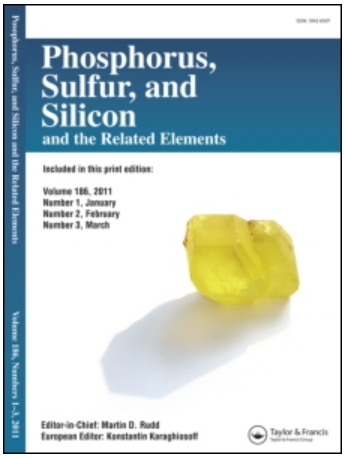

Phosphorus, Sulfur, and Silicon and the Related Elements
Publication details, including instructions for authors and subscription information:
http://www.informaworld.com/smpp/title~content=t713618290

Structural and Configurational Properties of Ethene, Silaethene, Germaethene, and Stannaethene: A Density Functional Theory Study and Natural Bond Orbital Analysis

Davood Nori-Shargh[ab]; Fahimeh Roohi[a]; Jila Farajzadeh[a]; Farzad Deyhimi[c]
[a] Chemistry Department, Islamic Azad University, Arak, Iran [b] Chemistry Department, Islamic Azad University, Tehran, Iran [c] Chemistry Department, Shahid Beheshti University, Evin, Tehran, Iran

To cite this Article Nori-Shargh, Davood , Roohi, Fahimeh , Farajzadeh, Jila and Deyhimi, Farzad(2007) 'Structural and Configurational Properties of Ethene, Silaethene, Germaethene, and Stannaethene: A Density Functional Theory Study and Natural Bond Orbital Analysis', Phosphorus, Sulfur, and Silicon and the Related Elements, 182: 4, 793 — 813
To link to this Article: DOI: 10.1080/10426500601059383
URL: http://dx.doi.org/10.1080/10426500601059383

Phosphorus, Sulfur, and Silicon, 182:793–813, 2007

ISSN: 1042-6507 print / 1563-5325 online
DOI: 10.1080/10426500601059383

Taylor & Francis
Taylor & Francis Group

Structural and Configurational Properties of Ethene, Silaethene, Germaethene, and Stannaethene: A Density Functional Theory Study and Natural Bond Orbital Analysis

Davood Nori-Shargh
Chemistry Department, Islamic Azad University, Arak, Iran; and Chemistry Department, Islamic Azad University, Hesarak, Poonak, Tehran, Iran

Fahimeh Roohi
Jila Farajzadeh
Chemistry Department, Islamic Azad University, Arak, Iran

Farzad Deyhimi
Chemistry Department, Shahid Beheshti University, Evin, Tehran, Iran

B3LYP/6-31G-B3LYP/3-21G,* and B3LYP/LANL2DZ**-based density functional theory (DFT) methods were used to investigate the ground-state structural and configurational properties of ethene (**1**), silaethene (**2**), germaethene (**3**), and stannaethene (**4**). All three methods showed that the ground-state structure of compounds **1–4** is planar. The results confirmed that the π bond energies (rotational barriers) are decreased from compound **1** to **4**. The double-bond rotation energy profiles show the existence of plane symmetrical intermediates, due to the pyramidalization at the silicon, germanium, and tin center in compounds **2–4**, respectively. Based on the B3LYP/6-31G*, B3LYP/3-21G* and B3LYP/LANL2DZ** optimized ground state geometries, the Natural Bond Orbital (NBO) analysis of donor-acceptor (bond-antibond) interactions revealed that the stabilization energies associated with the electronic delocalization from σ_{M-H} bonding orbitals to $\pi^*_{C=M}$ antibonding orbitals increase from compounds **1** to **4**. Also, the donor-acceptor interactions, as obtained from NBO analysis, could fairly explain the decrease of occupancies of σ_{M-H} bonding orbital and the increase of occupancies of $\pi^*_{C=M}$ antibonding orbitals from compounds **1** to **4**. Also, the NBO results showed that by increase of $\pi_{C=M} \rightarrow \sigma^*_{M-H}$ resonance*

Received July 27, 2006; accepted September 11, 2006.
Address correspondence to Davood Nori-Shargh, Chemistry Department, Science and Research Campus, Islamic Azad University, Hesarak, Poonak, Tehran, Iran. E-mail: nori_ir@yahoo.com

*energy in compounds **1–4**, the $\pi_{C=M}$ bonding orbital occupancies decrease, while the σ^*_{M-H}antibonding orbital occupancies increase. The results confirmed that by increase of $\sigma_{M-H} \rightarrow \pi^*_{C=M}$ and also $\pi_{C=M} \rightarrow \sigma^*_{M-H}$ resonance energies, the π bond energies (rotational barriers) decrease from compounds **1** to **4**. It has to be noted that the energy gap between $\pi_{C=M}$ bonding and $\pi^*_{C=M}$ antibonding orbitals decreased from compounds **1** to **4**.*

Keywords Ab initio; density functional theory; germaethene; Natural Bond Orbital; π bond energies; silaethene; stannaethene

INTRODUCTION

In most alkenes, the two double-bonded carbon atoms and their attached ligands are coplanar. It is well known that accepted orbital description involves sp2 hybridized carbon atoms for the C—C σ bond, linked to a π bond (p_π-p_π), formed by lateral overlap of the remaining p orbitals.[1] Double-bond energies are often divided into σ and π contributions, although directly measuring these quantities is impossible. However, ab initio methods afford an excellent way to assess these quantities. The C=C π bond in ethane is probably the most experimentally and theoretically investigated π bond.[2–5] A number of published papers have indicated that the triplet state and the rotated singlet state (which is usually referred to as the N state) represent a violation of Hund's rule.[6–9] In accordance with Hund's rule, the two unpaired π electrons should give the triplet ground state. It has to be noted that based on MCSCF/3-21G*, MCSCF/6-31G*, and SOCI/6-31G* calculations, Schmidt et al.[6] have reported that Hund's rule is violated in the rotation of C=C bond (e.g., a singlet structure lies below the rotational maxima on the triplet surface). Usually, the triplet structures lie 1–3 kcal mol^{-1} mol below the rotational maxima on the single surface.[6]

Effectively, B3LYP/6-31G*, B3LYP/3-21G*, and B3LYP/LANL2DZ** calculations performed in this work revealed that the energy values of transition states (TS) geometries for compounds **1–4** (with triplet spin multiplicity) were found to be lower than to those obtained with singlet spin multiplicity. It is interesting to note that for compounds **1–2**, the obtained B3LYP/6-31G*, B3LYP/3-21G*, and B3LYP/LANL2DZ** results (with triplet spin multiplicities) were also closer to the reported experimental data.[10–11] Therefore, this fact is in accordance with Hund's rule, which would predict that the triplet is below the rotated singlet state, as shown in Figure 1. Also, a number ab initio (SCF,[12,13] CI,[14] MCSCF,[6,15,16] GVB[4,7,11]) calculations have been performed to study the planar

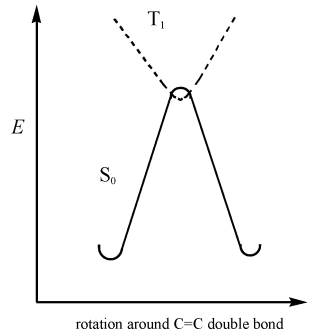

FIGURE 1 Potential energy surface profile of C=C double bond rotation with singlet and triplet states.

singlet and twisted triplet structures for ethene, silaethene, disilene, and their derivatives and isomers.

Note that there are not any reported data that show, particularly, the quantitative relationship between $\sigma_{M-H} \rightarrow \pi^*_{C=M}$ and also $\pi_{C=M} \rightarrow \sigma^*_{M-H}$ resonance energies and π bond energies (rotational barriers) in compounds **1–4** (see Scheme 1).

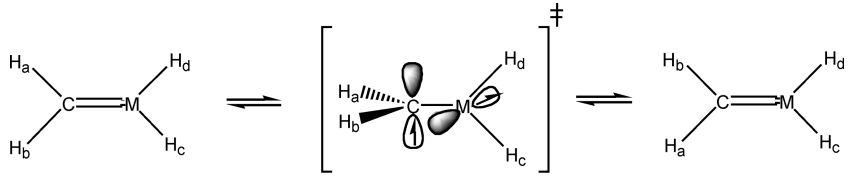

M=C (**1**), Si (**2**), Ge (**3**), Sn (**4**)

SCHEME 1

In this work, the stabilization energies (E_2) associated with $\sigma_{M-H} \rightarrow \pi^*_{C=M}$ and also $\pi_{C=M} \rightarrow \sigma^*_{M-H}$ delocalizations in compounds **1–4** were systematically and quantitatively investigated by the Natural Bond Orbital (NBO) analysis.[17,18] Using the GAUSSIAN 98 package of programs, the ground-state and transition-state structures of compounds **1–4** (see Scheme 1) have been optimized by the Density Functional Theory (DFT) based method at B3LYP/6-31G*, B3LYP/3-21G*, and B3LYP/LANL2DZ** levels of theory.[19–23] The B3LYP functional method combines Becke's three-parameter exchange function with the correlation function of Becke[20] and Lee et al.[21]

COMPUTATIONAL DETAILS

DFT calculations were carried out using B3LYP/6-31G*, B3LYP/3-21G*, and B3LYP/LANL2DZ** levels of theory with the GAUSSIAN 98 package of programs[19] implemented on a Pentium–PC computer with 1.7 GHz processor. Basis sets for atoms beyond the third row of the periodic table are usually handled somewhat differently. For these very large nuclei, electrons near the nucleus are treated in an approximate way, via Effective Core Potentials (ECPs). This treatment includes some relativistic effects, which are important in these atoms. For this purpose, the LANL2DZ is known to be one of the best of these basis sets.[19] It should be noted that, for all first row elements, the all-electron D95 double-zeta basis set (without ECP) is used in LANL2DZ. Therefore, in addition to B3LYP/6-31G* and B3LYP/3-21G* methods and in order to compare the effect of all-electron with pseudopotential basis sets, B3LYP/LANL2DZ** method was also used for the investigation of the configurational properties of compounds **1–4**. The MASSAGE keyword was further used in order to add an additional uncontracted polarization basis function to the LANL2DZ basis set for H, C, Si, Ge, and Sn atoms. The results obtained by B3LYP/6-31G* method concerning the configurational properties in compounds **1–3** were also compared at B3LYP/3-21G* and B3LYP/LANL2DZ** levels of theory. Initial estimation of the structural geometries of compounds **1–4** was obtained by a molecular mechanic program PCMODEL (88.0),[24] and for further optimization of geometries, PM3 method of MOPAC 7.0 computer program was used.[25,26] GAUSSIAN 98 program was finally used to perform DFT calculations at the B3LYP/6-31G* and B3LYP/3-21G* levels for compounds **1–3** and also B3LYP/LANL2DZ** level for compounds **1–4**. Energy minimum molecular geometries were located by minimizing energy, with respect to all geometrical coordinates without imposing any symmetrical constraints. The nature of the stationary points for compounds **1–4** has been fixed by means of the number of imaginary frequencies. For minimum state structures, only real frequency values, and in the transition-state, only single imaginary frequency value, were accepted.[27] Molecular transition state geometry structures were located by using the optimized geometry of the equilibrium molecular structures according to the procedure of Dewar et al. (keyword SADDLE).[28] These geometry structures were then reoptimized by QST3 option. The vibrational frequency of ground states and transition states were calculated by FREQ subroutine. For further optimization of the transition state structure, intrinsic reaction coordinate subroutine was also used. NBO analysis was then performed using B3LYP/6-31G*, B3LYP/3-21G*, and B3LYP/LANL2DZ** levels

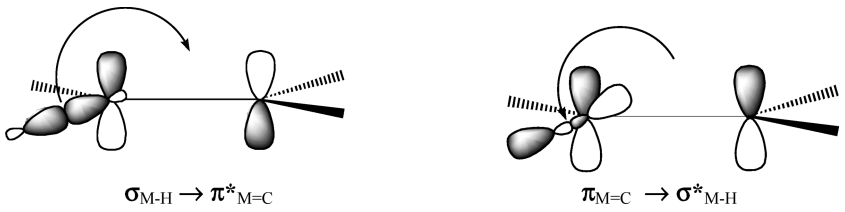

FIGURE 2 Schematic representation of delocalization between $\sigma_{M-H} \rightarrow \pi^*_{M=C}$ and $\pi_{M=C} \rightarrow \sigma^*_{M-H}$ bonding and antibonding orbitals.

by the NBO 3.1 program[17,18] included in the GAUSSIAN 98 package of programs.

RESULTS AND DISCUSSION

Corrected Zero Point (ZPE^c) and total electronic (E_{el}) energies ($E_o = E_{el} + ZPE^c$) for various conformations of compounds **1–3**, as calculated by the DFT-based method (B3LYP/6-31G* levels of theory) are given in Tables I. Table II shows the calculated Zero Point (ZPE) and total electronic (E_{el}) energies ($E_o = E_{el} + ZPE$) by B3LYP/3-21G* for various conformations of compounds **1–3**, and in Table III, the corresponding values for compounds **1–4**, as calculated by and B3LYP/LANL2DZ** method, are given. Also, NBO analysis was performed to calculate the σ_{M-H} bonding orbital and $\pi^*_{C=M}$ antibonding orbital occupancies for compounds **1–4** (M=C (**1**), Si (**2**), Ge (**3**) and Sn (**4**)), the resonance energies (E_2) associated with $\sigma_{M-H} \rightarrow \pi^*_{C=M}, \pi_{C=M} \rightarrow \sigma^*_{M-H}$ delocalizations (see Figures 2 and 3), and the energy gap between $\pi_{C=M}$ bonding and $\pi^*_{C=M}$ antibonding orbitals (see Tables IV–VI).

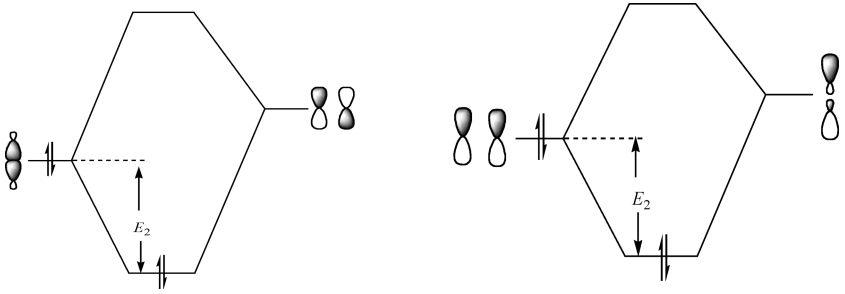

FIGURE 3 Schematic representation of stabilization energy (resonance energy) (E_2) from donor to acceptor for bonding and antibonding orbitals.

TABLE I Calculated Total Electronic Energies E_{el}, Zero-Point Energies *ZPE* (From B3LYP/6-31G* Level), and Relative Energies ΔE_o (E_h), (In Hartree), for the Ground and Transition State Geometries of the Double Bond Rotation Processes for Compounds 1–3

Compound	1		2			3		
Energies	D_{2h}	D_{2d}	$C_{2v(planar)}$	$C_{2v(perpendicular)}$	C_S	$C_{2v(planar)}$	$C_{2v(perpendicular)}$	C_S
ZPE[a]	0.050217	0.044783	0.039432	0.036500	0.037459	0.037747	0.0352248	0.035723
E_{el}	−78.587458	−78.485621	−329.941729	−329.876472	−329.887563	−2115.425920	−2115.364012	−2115.375602
E_o	−78.537241	−78.440838	−329.902297	−329.839972	−329.850104	−2115.388173	−2115.328787	−2115.339879
$\Delta E^b_{o(hartree)}$	0.000000	0.096403	0.000000	0.062325	0.052193	0.000000	0.059386	0.048294
$\Delta E^b_{o(kcalmol^{-1})}$	0.000000	60.493847	0.000000	39.109561	32.751629	0.000000	37.265183	30.304968

[a]Relative to the most stable form.
[b]Corrected by multiplying by a scaling factor (.9804).

TABLE II Calculated Total Electronic Energies E_{el}, Zero-Point Energies *ZPE* (from B3LYP/3-21G* Level) and Relative Energies ΔE_o (E_h), (in Hartree), for the Ground and Transition State Geometries of the Double Bond Rotation Processes for Compounds 1–3

Compound	1		2			3		
Energies	D_{2h}	D_{2d}	$C_{2v(planar)}$	$C_{2v(perpendicular)}$	C_S	$C_{2v(planar)}$	$C_{2v(perpendicular)}$	C_S
ZPE	0.051661	0.045847	0.040478	0.037471	0.038451	0.038683	0.0359160	0.036507
E_{el}	−78.161049	−78.055912	−328.284760	−328.217683	−328.228841	−2107.427397	−2107.366281	−2107.379374
E_o	−78.109388	−78.010065	−328.244282	−328.180212	−328.190391	−2107.388714	−2107.330365	−2107.342866
$\Delta E^a_{o(hartree)}$	0.000000	0.099323	0.000000	0.06407	0.053891	0.000000	0.058349	0.045848
$\Delta E^a_{o(kcalmol^{-1})}$	0.000000	62.326176	0.000000	40.204566	33.817141	0.000000	36.614581	28.770078

[a] Relative to the most stable form.

TABLE III Calculated Total Electronic Energies E_{el}, Zero-Point Energies *ZPE* (from B3LYP/LANL2DZ* Level) and Relative Energies ΔE_o (E_h), (in Hartree), for the Ground and Transition State Geometries of the Double Bond Rotation Processes for Compounds 1–4.

Compound	1		2			3			4		
Energies	D_{2h}	D_{2d}	$C_{2v(planar)}$	$C_{2v(perpendicular)}$	C_S	$C_{2v(planar)}$	$C_{2v(perpendicular)}$	C_S	$C_{2v(planar)}$	$C_{2v(perpendicular)}$	C_S
ZPE	0.051025	0.045697	0.040867	0.037258	0.038279	0.038964	0.036466	0.036697	0.036255	0.033837	0.034531
E_{el}	−78.600282	−78.500906	−44.358427	−44.261605	−44.270067	−44.222784	−44.144850	−44.158173	−43.805520	−43.743634	−43.760950
E_o	−78.549257	−78.455209	−44.317560	−44.224347	−44.231788	−44.183820	−44.108384	−44.121476	−43.769265	−43.709797	−43.726418
$\Delta E^a_{o(hartree)}$	0.000000	0.094048	0.000000	0.093213	0.085772	0.000000	0.075436	0.062344	0.000000	0.059468	0.042847
$\Delta E^a_{o\ (kcalmol^{-1})}$	0.000000	59.016060	0.000000	58.492090	53.822788	0.000000	47.336844	39.121483	0.000000	37.316765	26.886921

[a]Relative to the most stable form.

TABLE IV Calculated Bonding and Antibonding Orbital Occupancies, Stabilization (E_2), and Energy Gaps for the Ground State Geometries of Compounds 1–3, Using NBO Analysis Based on the Optimized Structures by B3LYP/3-21G* Level of Theory

Compound	1	2	3
Occupancies			
$\pi_{C=M}$	1.99474	1.98972	1.98034
$\pi^*_{C=M}$	0.00632	0.01714	0.03207
σ_{M-H}	1.98800	1.97979	1.96849
σ^*_{M-H}	0.00938	0.02198	0.03104
Stabilization Energies (Donor → Acceptor)			
$\sigma_{M-H} \rightarrow \pi^*_{C=M}$	1.52	3.76	7.31
$\pi_{C=M} \rightarrow \sigma^*_{M-H}$	1.20	2.01	4.53
Energy Gaps			
$\pi_{C=M}-\sigma^*_{M-H}$	1.22225	0.84128	0.78202
$\pi_{C=M}-\pi^*_{C=M}$	1.43138	0.88641	0.81699
$\sigma_{M-H} \rightarrow \sigma^*_{M-H}$	0.98834	0.71485	0.63211

B3LYP/6-31G* results show that the double bond rotational barriers for compounds **1–3** are 60.49, 39.11, and 37.27 kcal mol^{-1}, respectively. Also, based on B3LYP/3-21G* results, the required energies for the double bond rotations in compounds **1–3** are 62.33, 40.20, and 36.61 kcal

TABLE V Calculated Bonding and Antibonding Orbital Occupancies, Stabilization (E_2), and Energy Gaps for the Ground State Geometries of Compounds 1–3, Using NBO Analysis Based on the Optimized Structures by B3LYP/6-31G* Level of Theory.

Compound	1	2	3
Occupancies			
$\pi_{C=M}$	1.99651	1.99115	1.98343
$\pi^*_{C=M}$	0.00402	0.01465	0.02885
σ_{M-H}	1.98721	1.98128	1.97181
σ^*_{M-H}	0.00970	0.01915	0.02730
Stabilization Energies (Donor → Acceptor)			
$\sigma_{M-H} \rightarrow \pi^*_{C=M}$	0.96	3.17	6.07
$\pi_{C=M} \rightarrow \sigma^*_{M-H}$	0.94	1.68	3.94
Energy Gaps			
$\pi_{C=M}-\sigma^*_{M-H}$	1.21747	0.85213	0.81125
$\pi_{C=M}-\pi^*_{C=M}$	1.41434	0.90163	0.84874
$\sigma_{M-H}-\sigma^*_{M-H}$	0.99749	0.70436	0.66071

mol-1, respectively. The calculated energy barriers by B3LYP/6-31G* B3LYP/3-21G* levels of theory for compounds **1** and **2** are in good agreement with the previously reported experimental data.[10,11]

Also, B3LYP/LANL2DZ** results show that the double bond rotational barriers for compounds **1–4** are 59.02, 58.49, 47.34, and 37.32 kcal mol^{-1}, respectively. The decrease of double bond rotational barriers from compound **1** to **4**, as calculated by B3LYP/6-31G*, B3LYP/3-21G*, and B3LYP/LANL2DZ** levels of theory, are in good agreement with reported experimental[10,11] and theoretical results.[6–16]

Effectively, based on B3LYP/LANL2DZ** optimized structures, NBO analysis of donor-acceptor interactions showed that the resonance energy for $\sigma_{M-H} \rightarrow \pi^*_{C=M}$ delocalizations in compounds **1–4** are 0.66, 1.94, 5.09, and 6.59 kcal mol^{-1}, respectively (see Table VI). Also, based on the B3LYP/6-31G* optimized ground state geometries, the NBO analysis showed that $\sigma_{M-H} \rightarrow \pi^*_{C=M}$ resonance energies for compounds **1–3** are 0.96, 3.17, and 6.07 kcal mol^{-1}, respectively (see Table V). The $\sigma_{M-H} \rightarrow \pi^*_{C=M}$ resonance energies for compounds **1–3** are 1.52, 3.76, and 7.31 kcal mol^{-1}, respectively, as obtained from NBO analysis, based on the B3LYP/3-21G* optimized ground state geometries (see Table IV). Based on the B3LYP/3-21G* optimized ground state geometries for compounds **1–3**, the NBO results showed, as well, that $\sigma_{M-H} \rightarrow \pi^*_{C=M}$ resonance energies, are greater than those in B3LYP/6-31G* and B3LYP/LANL2DZ** optimized geometries (see Tables IV–VI).

TABLE VI Calculated Bonding and Antibonding Orbital Occupancies, Stabilization Energies (E_2), and Energy Gaps for the Ground State Geometries of Compounds 1–4, Using NBO Analysis Based on the Optimized Structures by B3LYP/LANL2DZ Level of Theory**

Compound	1	2	3	4
Occupancies				
$\pi_{C=M}$	1.99760	1.99585	1.98968	1.98228
$\pi^*_{C=M}$	0.00254	0.00625	0.01600	0.02615
σ_{M-H}	1.98480	1.98450	1.97539	1.96707
σ^*_{M-H}	0.01173	0.01494	0.02185	0.02615
Stabilization Energies (Donor → Acceptor)				
$\sigma_{M-H} \rightarrow \pi^*_{C=M}$	0.66	1.94	5.09	6.59
$\pi_{C=M} \rightarrow \sigma^*_{M-H}$	0.67	0.93	1.78	2.73
Energy Gaps				
$\pi_{C=M} - \sigma^*_{M-H}$	1.24696	0.85369	0.75798	0.62752
$\pi_{C=M} - \pi^*_{C=M}$	1.37671	1.12622	0.98022	0.78096
$\sigma_{M-H} - \sigma^*_{M-H}$	1.02506	0.71494	0.63883	0.53104

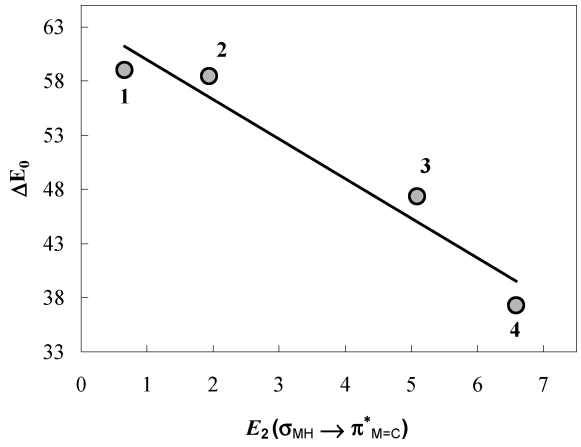

FIGURE 4 Calculated double bond rotational energy barrier (ΔE_o, in kcal mol^{-1}) for compounds **1–4**, plotted as a function of E_2 ($\sigma_{MH} \rightarrow \pi^*_{M=C}$).

The results revealed that by the increase of $\sigma_{M-H} \rightarrow \pi^*_{C=M}$, π bond rotation barrier heights ($\Delta E_o^{(1)a}$) decrease from compound **1** to compound **4** (see Figures 4 and 5 and Tables I–III and IV–VI).

On the other hand, based on B3LYP/LANL2DZ** optimized structures, the NBO analysis of donor-acceptor interactions showed that the resonance energy for $\pi_{C=M} \rightarrow \sigma^*_{M-H}$ delocalizations in compounds **1–4** are 0.67, 0.93, 1.78, and 2.73 kcal mol^{-1}, respectively (see Table VI). Also, based on the B3LYP/6-31G* optimized ground state geometries, the NBO analysis showed that the $\pi_{C=M} \rightarrow \sigma^*_{M-H}$ resonance energies for compounds **1–3** are 0.94, 1.68, and 3.94 kcal mol^{-1}, respectively (see Table V). The $\pi_{C=M} \rightarrow \sigma^*_{M-H}$ resonance energies for compounds **1–3** are 1.20, 2.01, and 4.53 kcal mol^{-1}, respectively, as obtained from NBO analysis, based on the B3LYP/3-21G* optimized ground state geometries (see Table IV). Similar to $\sigma_{M-H} \rightarrow \pi^*_{C=M}$ delocalizations, based on the B3LYP/3-21G* optimized ground state geometries, the NBO results showed that the $\pi_{C=M} \rightarrow \sigma^*_{M-H}$ resonance energies for compounds **1–3** are greater than those in B3LYP/6-31G* and B3LYP/LANL2DZ** optimized geometries (see Tables IV–VI). The results revealed that by an increase of $\pi_{C=M} \rightarrow \sigma^*_{M-H}$, the π bond rotation barrier heights ($\Delta E_o^{(2)b}$) decrease from compound **1** to compound **4** (see Figures 5 and 6 and Tables I–III and IV–VI). NBO results showed also that by increase of the $\sigma_{M-H} \rightarrow \pi^*_{C=M}$ and $\pi_{C=M} \rightarrow \sigma^*_{M-H}$ resonance energies in compounds **1–4**, the σ_{M-H} and $\pi_{C=M}$ bonding orbital occupancies decrease, while the σ^*_{M-H} and $\pi^*_{C=M}$ antibonding orbital occupancies increase (see Figures 7–10 and Tables IV–VI).

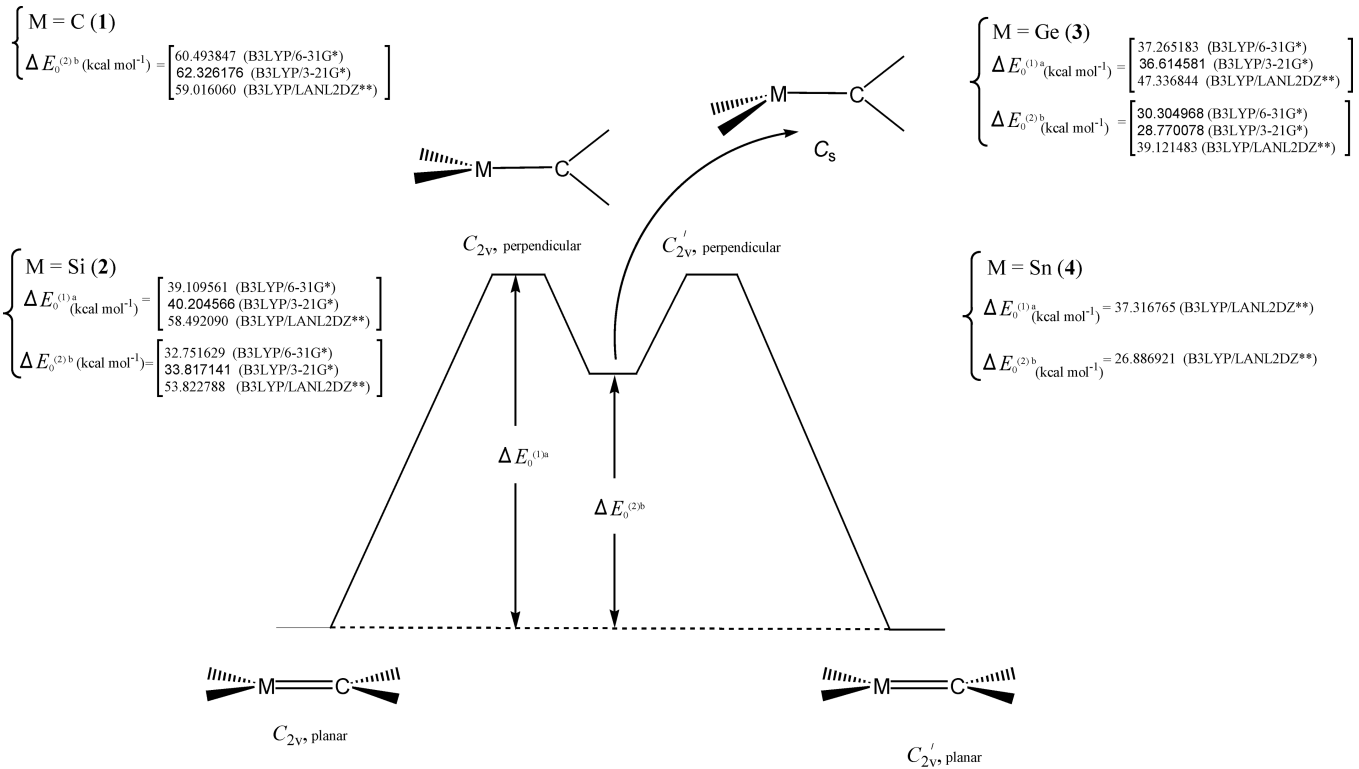

FIGURE 5 π bond rotation energy profile and atom pyramidalization for compounds **1–4**, as calculated by DFT-based methods (B3LYP/6-31G* B3LYP/3-21G* and B3LYP/LANL2DZ**).

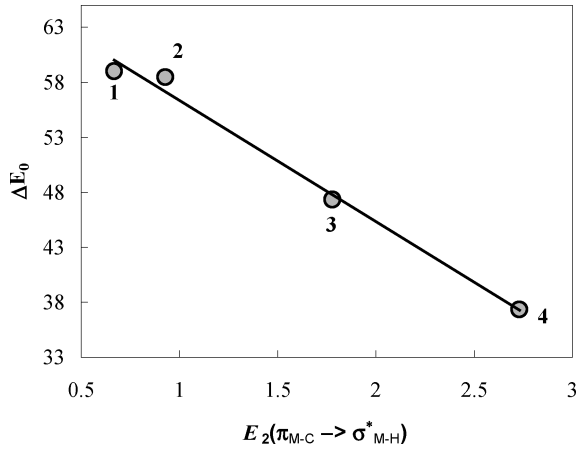

FIGURE 6 Calculated double bond rotational energy barrier (ΔE_o, in kcal mol^{-1}) for compounds **1–4**, plotted as a function of E_2 ($\pi_{M=C} \rightarrow \sigma*_{M-H}$).

Based on the B3LYP/LANL2DZ** optimized ground state geometries, the NBO results showed, as well, that the σ_{M-H} bonding orbital occupancies in compounds **1–4** are 1.98480, 1.98450, 1.97539, and 1.96707, respectively, while the σ^*_{M-H} antibonding orbital occupancies in compounds **1–4** are 0.01173, 0.01494, 0.02185, and 0.02615, respectively (see Table VI). The $\pi_{C=M}$ bonding orbital occupancies in compounds **1–4** are 1.99760, 1.99585, 1.98968, and 1.98228, respectively, while the $\pi^*_{C=M}$ antibonding orbital occupancies in compounds **1–4** are

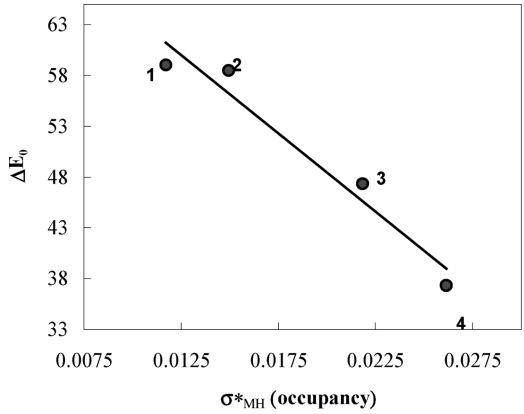

FIGURE 7 Calculated double bond rotational energy barrier (ΔE_o, in kcal mol^{-1}) for compounds **1–4**, plotted as a function of σ^*_{M-H} occupancy.

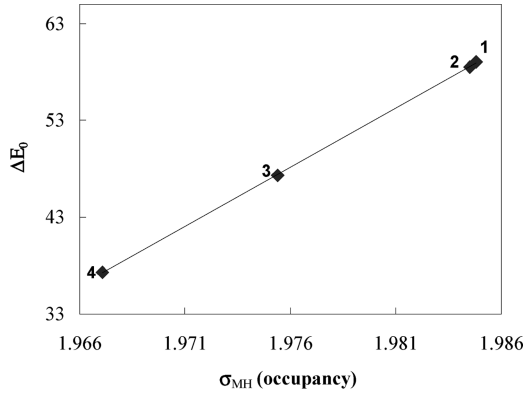

FIGURE 8 Calculated double bond rotational energy barrier (ΔE_o, in kcal mol^{-1}) for compounds **1–4**, plotted as a function of σ_{M-H} occupancy.

0.00254, 0.00625, 0.01600, and 0.02615, respectively, as obtained by NBO analysis based on the B3LYP/LANL2DZ** optimized ground state geometries (see Table VI). Using B3LYP/6-31G* and B3LYP/3-21G* levels of theory, similar trends are obtained for the increase of σ^*_{M-H} and $\pi^*_{C=M}$ and also for the decrease of σ_{M-H} and $\pi_{C=M}$ occupancies for compounds **1–3**. The results revealed also that by the increase of σ^*_{M-H} and $\pi^*_{C=M}$ and also by the decrease of σ_{M-H} and $\pi_{C=M}$ occupancies, the π bond rotation, barrier heights (ΔE_o) decrease from compound **1** to **4** (see Figures 7–10). It can be concluded that by the decrease of σ_{M-H}

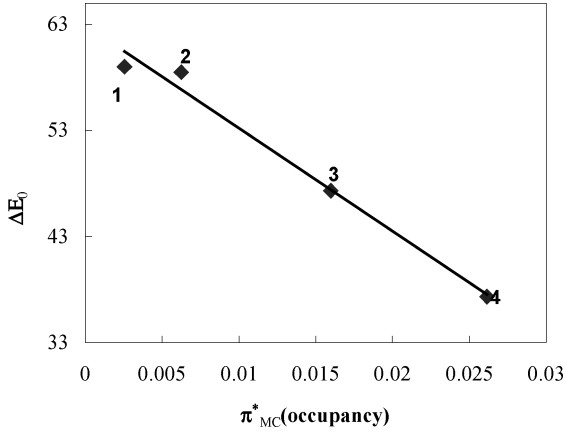

FIGURE 9 Calculated double bond rotational energy barrier (ΔE_o, in kcal mol^{-1}) for compounds **1–4**, plotted as a function of π^*_{MC} occupancy.

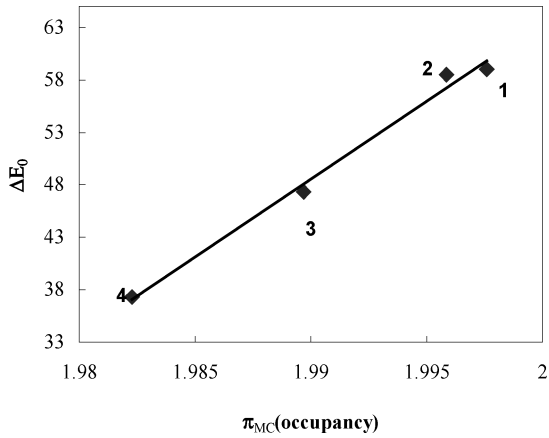

FIGURE 10 Calculated double bond rotational energy barrier (ΔE_o, in kcal mol^{-1}) for compounds **1–4**, plotted as a function of π_{MC} occupancy.

and $\pi_{C=M}$ bonding and the increase of σ^*_{M-H} and $\pi^*_{C=M}$ antibonding orbital occupancies in compounds **1–4**, the strength of the C=M double bonds decrease. This fact could fairly explain the increase of the C=M bond length from compound **1** to **4** (see Tables VII–IX). The results suggest also that in compounds **1–4**, the π bond rotation barrier heights are controlled by $\sigma_{M-H} \rightarrow \pi^*_{C=M}$ and $\pi_{C=M} \rightarrow \sigma^*_{M-H}$ resonance energies. It can be seen that by the increase of $\sigma_{M-H} \rightarrow \pi^*_{C=M}$ and $\pi_{C=M} \rightarrow \sigma^*_{M-H}$ delocalizations, the π bond rotation could take place more easily from compound **4** to **1**, respectively (see Figures 4 and 6). Therefore, the π bond rotation process in compound **4** is faster than in **3**, in compound **3** it is faster than in compound **2**, and also in compound **2** it is faster than in compound **1**.

Representative structural parameters for compounds **1–3**, as calculated by B3LYP/3-1G* and B3LYP/6-31G* levels of theory, are given in Tables VII and VIII, respectively, and B3LYP/LANL2DZ** calculated structural parameters for compounds **1–4** are given in Table IX. B3LYP/6-31G* results showed that the C=M double bond length values in compounds **1–3** are 1.331, 1.710, and 1.776 Å, respectively, while the C=M double bond length values in compounds **1–4**, as calculated by B3LYP/LANL2DZ** level of theory, are 1.339, 1.695, 1.784, and 1.955 Å (see Table IX), respectively. It also has to be noted that, as the M=C (M=C (1), Si (2), Ge (3), and Sn(4)) double bond lengths increase (see Tables VII–IX), the barrier heights for π bond rotation ($\Delta E_0^{(1)a}$) decrease (see Tables I–III).

TABLE VII B3LYP/3-21G* Calculated Structural Parameters for the Ground and Transition State Geometries for Compounds 1–3.

	1		2			3		
Compound	D_{2h}	D_{2d}	$C_{2v(planar)}$	$C_{2v(perpendicular)}$	C_S	$C_{2v(planar)}$	$C_{2v(perpendicular)}$	C_S
Bond Length (Å)								
r_{C-M}	1.329	1.453	1.710	1.872	1.851	1.792	1.944	1.954
r_{M-H}	1.086	1.089	1.478	1.479	1.495	1.544	1.541	1.571
Bond angles (°)								
θ_{H-C-M}	121.9	121.7	122.5	122.4	122.7	121.4	121.3	121.7
θ_{H-M-H}	116.2	116.6	114.8	119.7	107.7	114.8	119.2	107.6
Torsion angles (°)								
$\phi_{H4-C-M-H5}$	0.0	90.0	0.0	90.0	119.2	0.0	90.0	119.6
$\phi_{H4-C-M-H6}$	180.0	90.0	180.0	90.0	60.8	180.0	90.0	60.4
$\phi_{H4-H3-C-M}$	180.0	180.0	180.0	180.0	124.1	180.0	180.0	121.5

TABLE VIII B3LYP/6-31G* Calculated Structural Parameters for the Ground and Transition State Geometries for Compounds 1-3

	1		2			3		
Compound	D_{2h}	D_{2d}	$C_{2v(planar)}$	$C_{2v(perpendicular)}$	C_S	$C_{2v(planar)}$	$C_{2v(perpendicular)}$	C_S
Bond Length (Å)								
r_{C-M}	1.331	1.451	1.710	1.877	1.856	1.776	1.915	1.922
r_{M-H}	1.088	1.090	1.479	1.481	1.497	1.532	1.524	1.560
Bond Angles (°)								
θ_{H-C-M}	121.9	121.9	122.4	122.5	122.8	121.6	122.1	122.1
θ_{H-M-H}	116.2	116.2	114.8	119.6	107.7	114.7	118.4	107.4
Torsion Angles (°)								
$\phi_{H4-C-M-H5}$	0.0	90.0	0.0	90.0	119.2	0.0	90.0	119.7
$\phi_{H4-C-M-H6}$	180.0	90.0	180.0	90.0	60.8	180.0	90.0	60.3
$\phi_{H4-H3-C-M}$	180.0	180.0	180.0	180.0	124.1	180.0	180.0	122.5

TABLE IX B3LYP/LANL2DZ Calculated Structural Parameters for the Ground and Transition State Geometries for Compounds 1–4**

	1		2			3			4		
Compound	D_{2h}	D_{2d}	$C_{2v(planar)}$	$C_{2v(perpendicular)}$	C_S	$C_{2v(planar)}$	$C_{2v(perpendicular)}$	C_S	$C_{2v(planar)}$	$C_{2v(perpendicular)}$	C_S
Bond Length (Å)											
r_{C-M}	1.339	1.453	1.695	1.875	1.865	1.784	1.887	1.948	1.955	2.101	2.121
r_{M-H}	1.088	1.089	1.455	1.478	1.494	1.526	1.527	1.561	1.693	1.728	1.735
Bond Angles (°)											
θ_{H-C-M}	121.7	121.7	122.5	122.2	122.5	121.7	122.1	122.1	121.8	122.2	122.4
θ_{H-M-H}	116.7	116.6	115.1	119.4	108.4	115.1	114.2	107.2	114.0	120.1	106.1
Torsion Angles (°)											
$\phi_{H4-C-M-H5}$	0.0	90.0	0.0	90.0	118.4	0.0	90.0	119.9	0.0	90.0	121.6
$\phi_{H4-C-M-H6}$	180.0	90.0	180.0	90.0	61.6	180.0	90.0	60.1	180.0	90.0	58.4
$\phi_{H4-H3-C-M}$	180.0	180.0	180.0	180.0	125.5	180.0	180.0	121.5	180.0	180.0	118.5

It has to be noted that for compounds **2–4**, all used methods (B3LYP/6-31G*, B3LYP/3-21G*, and B3LYP/LANL2DZ**) show the existence of plane symmetrical intermediates in their double bond rotation energy profiles due to the pyramidalization at the silicon, germanium, and tin center, respectively (see Figure 5). These plane symmetrical intermediates for compounds **2–3** are found to be higher in energy than their ground state structures about 32.75 and 30.30 kcal mol^{-1}, as calculated by B3LYP/6-31G* method. Also, B3LYP/3-21G* results show that the corresponding energy value for the plane symmetrical intermediate for compounds **2–3** are found to be 33.82 and 28.77 kcal mol^{-1} higher in energy (than their ground state structures), respectively. Further, the corresponding energy value for the plane symmetrical intermediate for compound **4** (e.g., tin center pyramidalization) is found to be 26.89 kcal mol^{-1} higher in energy, as calculated by B3LYP/LANL2DZ** level of theory.

CONCLUSION

NBO analysis and DFT methods used in this work provided a useful picture, both from bonding and configurational properties for compounds **1–4**. B3LYP/6-31G*, B3LYP/3-21G*, and B3LYP/LANL2DZ** results showed that the ground state structure of compounds **1–4** is planar, and the π bond energies (rotational barriers) decrease from compound **1** to **4**. The double bond rotation energy profiles showed the existence of plane symmetrical intermediates, due to the pyramidalization at the silicon, germanium, and tin center in compounds **2–4**, respectively. All used methods (B3LYP/6-31G*, B3LYP/3-21G*, and B3LYP/LANL2DZ**) showed that these plane symmetrical intermediates for compounds **2–4** are about 26–34 kcal mol^{-1} higher in energy than their ground state structures. Based on the optimized ground state geometries using B3LYP/6-31G*, B3LYP/3-21G*, and B3LYP/LANL2DZ** methods, the NBO analysis of donor-acceptor (bond-antibond) interactions revealed that the stabilization energies associated with the electronic delocalization from σ_{M-H} bonding orbitals to $\pi^*_{C=M}$ antibonding orbitals increase from compounds **1** to **4**. The donor-acceptor interactions, as obtained from NBO analysis, could fairly explain the decrease of occupancies of σ_{M-H} bonding orbital and the increase of occupancies of $\pi^*_{C=M}$ antibonding orbitals from compounds **1** to **4**. Further, the NBO results showed that by increase of $\pi_{C=M} \rightarrow \sigma^*_{M-H}$ resonance energy in compounds **1–4**, the $\pi_{C=M}$ bonding orbital occupancies decrease, while σ^*_{M-H} antibonding orbital occupancies increase. The results revealed that by the increase of $\sigma_{M-H} \rightarrow \pi^*_{C=M}$ and also $\pi_{C=M} \rightarrow \sigma^*_{M-H}$ resonance energies, the π bond

energies (rotational barriers) decrease from compounds **1** to **4**. It has to be noted that the energy gap between $\pi_{C=M}$ bonding and $\pi^*_{C=M}$ antibonding orbitals decrease from compounds **1** to **4**. The decrease of energy gap between $\pi_{C=M}$ bonding and $\pi^*_{C=M}$ antibonding orbitals could explain the decrease of π bond energies (rotational barrier energies).

REFERENCES

[1] E. L. Eliel and S. H. Wilen, *Stereochemistry of Organic Compounds* (Wiley, New York, 1994) and references therein.
[2] W. J. Pietro and W. J. Hehre, *J. Am. Chem. Soc.*, **104,** 16 (1982).
[3] O. P. Strausz, M. A. Robb, G. Theodorakopoulos, P. G. Mezey, and I. G. Csizmadia, *Chem. Phys. Letters.*, **48**, 162 (1977).
[4] Y. Wang and R. A. Poirier, *Can. J. Chem.*, 76 (1998).
[5] S. Bailleux, M. Bogey, J. Demaison, H. Burger, M. Senzlober, J. Breidung, et al., *J. Chem. Phys.*, 24 (1997).
[6] M. W. Schmidt, P. N. Truong, and M. S. Gordon., *J. Am. Chem. Soc.*, **109,** 5217 (1987).
[7] F. Voter, M. M. Goodgame, and W. A. Goddard III., *Chem. Phys.*, **98,** 7 (1985).
[8] Y. Yamaguchi, Y. Osamura, and H. F. Schaefer III, *J. Am. Chem. Soc.*, **105,** 7506 (1983).
[9] R. J. Buenker and S. D. Peyerimhoff, *Chem. Phys.*, **9,** 75 (1976).
[10] J. E. Douglas, B. S. Rabinovitch, and F. S. Looney, *J. Chem. Phys.*, **23,** 315 (1955).
[11] S. K. Shin, K. K. Irikura, J. L. Beauchamp, and W. A. Goddard III, *J. Am. Chem. Soc.*, **110,** 24 (1988).
[12] K. D. Dobbs and W. J. Hehre, *Organometallics*, **5,** 2057 (1986).
[13] (a) R. A. Poirier and J. D. Goddard, *Chem. Phys. Lett.*, **80,** 37 (1981); (b) H. J. Kohler, *Chem. Phys. Lett.*, **85,** 467 (1982); (c) Y. Yoshioka, J. D. Goddard, and H. F. Schaefer III, *J. Am. Chem. Soc.*, **103,** 2452 (1981); (d) D. A. Dixon, T. Fukunaga, and B. E. Smart, *J. Am. Chem. Soc.*, **108,** 1585 (1986).
[14] B. R. Brook and H. F. Scheafer III, *J. Am. Chem. Soc.*, **101,** 307 (1979); (b) J. D. Goddard, Y. Yoshioka, and H. F. Scheafer III, *J. Am. Chem. Soc.*, **102,** 7647 (1980).
[15] D. A. Hrovat, H. Sun, and W. T. Bordon, *J. Mol. Struct. (Theochem),* **163,** 51 (1988).
[16] (a) H. J. Kohler and H. Lischka, *J. Am. Chem. Soc.*, **104,** 5884 (1982); (b) M. W. Schmidt, M. S. Gordon, and M. Dupuis, *J. Am. Chem. Soc.*, **107,** 2585 (1985).
[17] E. D. Glendening, A. E. Reed, J. E. Carpenter, and F. Weinhold, in Gaussian 98, NBO Version 3.1, Gaussian Inc., Pittsburg, PA.
[18] E. Reed, L. A. Curtiss, and F. Weinhold, *Chem. Rev.*, **88,** 899 (1988).
[19] M. J. Frisch, G. W. Trucks, H. B. Schlegel, G. E. Scuseria, M. A. Robb, J. R. Cheeseman, et al., GAUSSIAN 98 (Revision A.3), Gaussian Inc., Pittsburgh, PA, USA, 1998.
[20] A. D. Becke, *J. Chem. Phys.*, **98,** 5648 (1993).
[21] C. Lee, W. Yang, and R. G. Parr, *Phys. Rev., B*, **37,** 785 (1988).
[22] W. J. Hehre, L. Radom, P. V. R. Schleyer, and J. A. Pople, *Ab initio Molecular Orbital Theory* (Wiley, New York, 1986).
[23] J. M. Seminario and P. Politzer (Eds.), *Modern Density Function Theory, A Tool for Chemistry* (Elsevier, Amsterdam, 1995).
[24] Program available from Serena Software, P.O. Box 3076, Bloomington, IN 47402-3076, USA.

[25] J. J. P. Stewart, *QCPE* 581, Department of Chemistry, Indiana University, Bloomington, IN, USA.
[26] J. J. P. Stewart, *J. Comput.-Aided Mol. Des.*, **4,** 1 (1990).
[27] (a) J. W. McIver, Jr., *Acc. Chem. Res.*, **7,** 72 (1974); (b) O. Ermer, *Tetrahedron*, **31,** 1849 (1975).
[28] M. J. S. Deware, E. F. Heally, and J. J. P. Stewart, *J. Chem. Soc. Faraday Trans.*, **80,** 227 (1984).